Inorg. Chem. **2004**, *43*, 1021–1030

Self-Assembly of Cu^{II} and Ni^{II} [2 × 2] Grid Complexes and a Binuclear Cu^{II} Complex with a New Semiflexible Substituted Pyrazine Ligand: Multiple Anion Encapsulation and Magnetic Properties

Dilovan S. Cati,[†] Joan Ribas,[‡] Jordi Ribas-Ariño,[§] and Helen Stoeckli-Evans*[,†]

Institut de Chimie, Université de Neuchâtel, Avenue Bellevaux 51, Case Postale 2, CH-2007 Neuchâtel, Switzerland, Departament de Química Inorgànica, Universitat de Barcelona, Diagonal 647, 08028 Barcelona, Spain, and Departament de Química Física, Universitat de Barcelona, Diagonal 647, 08028 Barcelona, Spain

Received May 28, 2003

With the new substituted pyrazine ligand pyrazine-2,3-dicarboxylic acid bis[(pyridin-2-ylmethyl)amide], H_2L, a binuclear complex $[Cu_2(LH)(Cl_3)(H_2O)]\cdot H_2O$ (**1**) and two [2 × 2]G grid complexes, $\{[Cu_4(LH)_4](ClO_4)_4\}\cdot 5CH_3OH\cdot 4H_2O$ (**2**) and $\{[Ni_4(LH)_4]Cl_4\}\cdot 5CH_3CN\cdot 13H_2O$ (**3**), have been synthesized and characterized spectroscopically and crystallographically. The ligand H_2L crystallized in the triclinic space group $P\bar{1}$, with $a = 4.9882(7)$ Å, $b = 12.079(2)$ Å, $c = 14.454(2)$ Å, $\alpha = 107.08(2)°$, $\beta = 98.61(2)°$, $\gamma = 97.54(2)°$, $V = 808.8(2)$ Å^3, $Z = 2$, R1 = 0.0747, and $R_w = 0.1829$ for 1319 observed reflections [$I > 2\sigma(I)$]. The molecule is L-shaped with a strong intramolecular bifurcated hydrogen bond in half of the molecule. In the crystal the molecules are linked by an intermolecular hydrogen bond to form a 1D polymer. The binuclear complex $[Cu_2(LH)(Cl_3)(H_2O)]\cdot H_2O$ (**1**) crystallized in the monoclinic space group $P2_1/a$, with $a = 8.6859(7)$ Å, $b = 28.060(2)$ Å, $c = 9.5334(9)$ Å, $\beta = 107.89(1)°$, $V = 2211.2(3)$ Å^3, $Z = 4$, R1 = 0.039, and $R_w = 0.097$ for 1408 observed reflections [$I > 2\sigma(I)$]. There are two independent copper atoms both having square pyramidal geometry. Both coordinate to a pyrazine, a pyridine, and an amide N atom. Two chlorines complete the coordination sphere of one of the copper atoms, while one chlorine atom and a water molecule complete the coordination sphere of the other. The copper(II) [2 × 2] grid complex $\{[Cu_4(LH)_4](ClO_4)_4\}\cdot 5CH_3OH\cdot 4H_2O$ (**2**) crystallized in the triclinic space group $P\bar{1}$, with $a = 17.1515(14)$ Å, $b = 17.7507(13)$ Å, $c = 19.3333(15)$ Å, $\alpha = 67.34(1)°$, $\beta = 69.79(1)°$, $\gamma = 71.50(1)°$, $V = 4980.3(7)$ Å^3, $Z = 2$, R1 = 0.083, and $R_w = 0.207$ for 5532 observed reflections [$I > 2\sigma(I)$]. The four Cu^{II} atoms are octahedrally coordinated by two pyrazine, two pyridine, and two amide N atoms and occupy the corners of a [2 × 2] grid with edge lengths, Cu···Cu, varying from 7.01 to 7.39 Å. The nickel(II) [2 × 2] grid complex $\{[Ni_4(LH)_4]Cl_4\}\cdot 5CH_3CN\cdot 13H_2O$ (**3**) crystallized in the monoclinic space group $C2/c$, with $a = 16.3388(10)$ Å, $b = 29.754(2)$ Å, $c = 20.857(1)$ Å, $\beta = 101.845(1)°$, $V = 9923.6(12)$ Å^3, $Z = 4$, R1 = 0.050, and wR2 = 0.101 for 3391 observed reflections [$I > 2\sigma(I)$]. Here the complex possesses C_2 symmetry and again each metal atom is octahedrally coordinated to two pyrazine, two pyridine, and two amide N atoms. They occupy the corners of a [2 × 2] grid with an average edge length, Ni···Ni, of 6.97 Å. Of the four anions (ClO_4^-'s in **2** and Cl^-'s in **3**) required to equilibrate the charges in the grid complexes, two are encapsulated, one above and one below the plane of the four metal atoms. The remaining two anions are located between the "wings" of the ligands. Magnetic susceptibility measurements indicate that the binuclear complex **1** is antiferromagnetic, with a J value of –15.07 cm^{-1}. This is larger than the J values found for the Cu^{II} (**2**) and Ni^{II} (**3**) grid complexes, which were –5.87 and –2.64 cm^{-1}, respectively. DFT calculations have been carried out to explain the difference in the J values found for complexes **1** and **2**.

Introduction

One of the major goals in inorganic supramolecular chemistry today is the self-assembly of polynuclear coordination arrays. The design of suitable ligands, and the choice of metal ions, to generate well-defined architectures in a controlled fashion, comprise an extremely active field of research.[1] The presence of metal ions in such coordination arrays may result in the development of many varied

* To whom correspondence should be addressed. E-mail: helen.stoeckli-evans@unine.ch.
[†] Institut de Chimie, Université de Neuchatel.
[‡] Departament de Química Inorgànica, Universitat de Barcelona.
[§] Departament de Química Física, Universitat de Barcelona.

10.1021/ic030174s CCC: $27.50
Published on Web 01/14/2004

Scheme 1

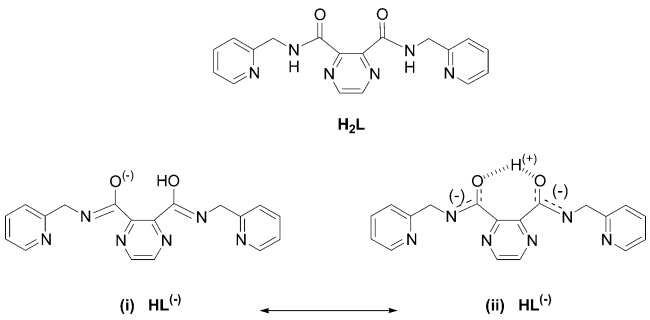

physicochemical properties such as electrochemical, optical, magnetic, mechanical, and catalytic activity.[2] Polynucleating ligands with continuous coordination pockets arranged in a linear fashion can align metal ion centers in chains[3] or grids,[4] depending on the chelate ring sizes involved and the coordination sphere of the metals used. For grids, the ligands used are normally planar and contain rigid linear spacers between the binding sites. Bidentate heteroaromatic linkers, such as pyrimidines or pyridazines, have commonly been used[2] and resulted in the formation of [2 × 2]G,[4c,d,g] [2 × 3]G,[4e] and [3 × 3]G[4f,j,i] grids. Although most of these grids are of diamagnetic metals, such as Ag^{I} and Cu^{I}, some contain paramagnetic centers, such as Cu^{II},[4i−5] Mn^{II},[4j] Ni^{II},[4k] and Co^{II}.[4b,d,6] In general antiferromagnetic intramolecular coupling was observed except in some cases of Cu^{II} where ferromagnetic coupling, associated with orthogonal magnetic connections, prevails.[4h,i]

Here we describe the new semiflexible ligand pyrazine-2,3-dicarboxylic acid bis[(pyridin-2-ylmethyl)amide] (H_2L; Scheme 1) and its coordination chemistry with copper(II) and nickel(II), with multiple anion encapsulation. The complexes formed were characterized spectroscopically and crystallographically, and their magnetic properties were also examined.

Experimental Section

General Procedures. All chemicals were used as received without further purification. Infrared spectra of the complexes were obtained using a Perkin-Elmer FT-IR 1720X spectrometer with KBr pellets. For H_2L the IR spectra were obtained in a CH_2Cl_2 solution and as KBr pellets. The absorption bands are given in cm^{-1}, and all spectra were taken in the range between 4000 and 400 cm^{-1}. ^1H NMR and ^{13}C NMR measurements were carried out on a Bruker AMX 400 FTP spectrometer in DMSO-d_6. C, H, and N microanalysis were carried out by the Ecole d'Ingénieur, Fribourg, Switzerland. The ESI-MS spectra were performed using a Bruker FTMS 4.7T BioAPEX II by the MS-Service at the Institute of Organic Chemistry, University of Fribourg. The melting points were obtained with a BUCHI 510 melting point apparatus.

The magnetic measurements were carried out on powder samples (40.85, 48.72, and 51.34 mg, for the complexes **1**−**3**, respectively) with a pendulum type magnetometer−susceptometer (MANICS DSM-8) equipped with an Oxford helium continuous-flow cryostat, working in the 4.2−300 K range and a Drusch EAF 16UE electromagnet. The magnetic field was approximately 0.1 T. The diamagnetic corrections were evaluated from Pascal's tables.

Caution! *Perchlorate salts are potentially explosive and should only be used in small quantities and handled with the necessary precautions*.

Synthesis. The ligand pyrazine-2,3-dicarboxylic acid bis[(pyridin-2-ylmethyl)amide], H_2L, was prepared by refluxing 3.92 g (20 mmol) of the dimethyl ester of pyrazine-2,3-dicarboxylic acid[7] and an excess of 2-(aminomethyl)pyridine (5.41 g, 50 mmol) in 15 mL of methanol for 8 h. After evaporation of the methanol a yellowish oil remained. The excess of 2-(aminomethyl)pyridine was eliminated by column chromatography on silica gel using CH_2Cl_2 as eluent. The crude compound was then recrystallized using a mixture of 50 mL of ethyl acetate and 3 mL of dichloromethane to give colorless crystals; mp 141 C°. Yield: 5.62 g, 81%. ^1H NMR (400 MHz, ppm, DMSO-d_6): 9.28 (t, 1H, $J_{hg} = 6.0$, H_h); 8.86 (s, 1H, $H_n = H_m$); 8.52 (ddd, 1H, $J_{bc} = 4.8$, $J_{bd} = 1.7$, $J_{be} = 0.9$, H_b); 7.76 (td, 1H, $J_{dc} = 7.6$, $J_{db} = 1.8$, H_d); 7.50 (d, 1H, $J_{ed} = 7.9$, H_e); 7.28 (ddd, 1H, $J_{cd} = 7.8$, $J_{cb} = 4.8$, $J_{ce} = 7.5$, H_c); 4.60 (d, 2H, $J_{gh} = 6.0$, H_g). ^{13}C NMR (400 MHz, ppm, DMSO-d_6): 165.6, 158.9, 149.6, 147.5, 145.6, 137.6, 123.0, 121.9, 45.2. Anal. Calcd for $C_{18}H_{16}N_4O_2$ ($M_r = 348.36$): C, 62.06; H, 4.63; N, 24.12. Found: C, 62.11; H, 4.63; N, 24.17.

$[Cu_2(LH)(Cl_3)(H_2O)]\cdot H_2O$ (1). A 0.054 g amount of H_2L (0.156 mmol) was added to a solution of $CuCl_2\cdot 2H_2O$ (0.053 g; 0.312 mmol) in 15 mL of ethanol. The solution was refluxed for 1.5 h. The resulting precipitate (same color as $CuCl_2\cdot 2H_2O$) was filtered out and washed with 10 mL of ethanol. This crude product was dissolved in 13 mL of water, 6 mL of ethanol was added, and the mixture was refluxed for 2.5 h. The resulting blue-turquoise solution was filtered and the solution allowed to evaporate slowly, giving finally very small green blocklike crystals (yield: 68 mg, 73%), which on exposure to air slowly became opaque. Anal. Calcd for $Cu_2C_{18}H_{17}Cl_3N_6O_3$: C, 36.16; H, 2.70; N, 14.06. Found: C, 36.45; H, 2.83; N, 13.33.

(1) (a) Lehn, J. M. *Supramolecular Chemistry. Concept and Perspectives*; VCH: Weinheim, Germany, 1995; Chapter 9. (b) Caulder, D. L.; Raymond, K. N. *Acc. Chem. Res*. **1999**, *32*, 975. (c) Leininger, S.; Olenyuk, B.; Stang, P. J. *Chem. Rev*. **2000**, *100*, 853. (d) Cotton, F. A.; Lin, C.; Murillo, C. A. *Acc. Chem. Res*. **2001**, *34*, 759. (e) Evans, O. R.; Lin, W. *Acc. Chem. Res*. **2002**, *35*, 511.

(2) Swiegers, G. F.; Malefetse, T. J. *Chem. Rev*. **2000**, *100*, 3483.

(3) (a) Cotton, F. A.; Daniels, L. M.; Lu, T.; Murillo, C. A.; Wang, X. J. *Chem. Commun*. **1999**, 517. (b) Wang, C. C.; Lo, W. C.; Chou, C. C.; Lee, G. H.; Chen, J. M.; Pend, S. M. *Inorg. Chem*. **1998**, *37*, 4059. (c) van Albada, G. A.; Mutikainen, I.; Turpeinen, U.; Reedijk, J. *Eur. J. Inorg. Chem*. **1998**, 547.

(4) (a) Waker, P. N.; Lehn, J. M.; Fisher, J.; Youinou, M. T. *Angew. Chem. Ed. Engl*. **1994**, *33*, 2284. (b) Duan, C. Y.; Liu, Z. H.; You, X.-Z.; Xue, F.; Mak, T. C. W. *Chem. Commun*. **1997**, 381−82. (c) Baxter, P. N. W.; Lehn, J. M.; Kneisel B. O.; Fenske. D. *Chem. Commun*. **1997**, 2231. (d) Hanan, G. S.; Volkmer, D.; Schubert, U. S.; Lehn, J. M.; Baum, G.; Frenske, D. *Angew. Chem., Int. Ed. Engl*. **1997**, *36*, 1842. (e) Baxter, P. N. W.; Lehn, J. M.; Kneisel B. O.; Fenske. D. *Angew. Chem., Int. Ed. Engl*. **1997**, *36*, 1978. (f) Suenaga, Y.; Tan, S. G.; Wu, L. P.; Ino, I.; Kuroda-Sowa, T.; Maezawa, M.; Musajata, M. *J. Chem. Soc., Dalton Trans*. **1998**, 1121. (g) Bassani, D. M.; Lehn, J. M.; Fromm, K.; Fenske, D. *Angew. Chem., Int. Ed*. **1998**, *37*, 2364. (h) Matthews, C. J.; Avery, K.; Xu, Z.; Thompson, L. K.; Zhao, L.; Miller, D. O.; Biradha, K.; Poirier, K.; Zaworotko, M. J.; Wilson, C.; Goeta, A. E.; Howard, J. A. K. *Inorg. Chem*. **1999**, *38*, 5266. (i) Zhao, L.; Xu, Z.; Thompson, L. K.; Heath, S. L.; Miller, D. O.; Ohba, M. *Angew. Chem., Int. Ed*. **2000**, *39*, 3114. (j) Zhao, L.; Matthews, C. J.; Thompson, L. K.; Heath, S. L. *Chem. Commun*. **2000**, 265. (k) Cheng, H.; Ying, D. C.; Jie, F. C.; Jiang, L. Y.; Jin, M. Q. *J. Chem. Soc., Dalton Trans*. **2000**, 1207.

(5) Waldmann, O.; Koch, R.; Schromm, S.; Müller, P.; Zhao, L.; Thompson, L. K. *Chem. Phys. Lett*. **2000**, *332*, 73.

(6) Waldmann, O.; Hassmann, J.; Müller, P.; Hanan, G. S.; Volkmer, D.; Schubert, U. S.; Lehn, J. M. *Phys. Rev. Lett*. **1997**, *78*, 3390.

(7) Schut, W. J.; Mager, H. I. X.; Berends, W. *Inorg. Chem*. **1961**, *80*, 391.

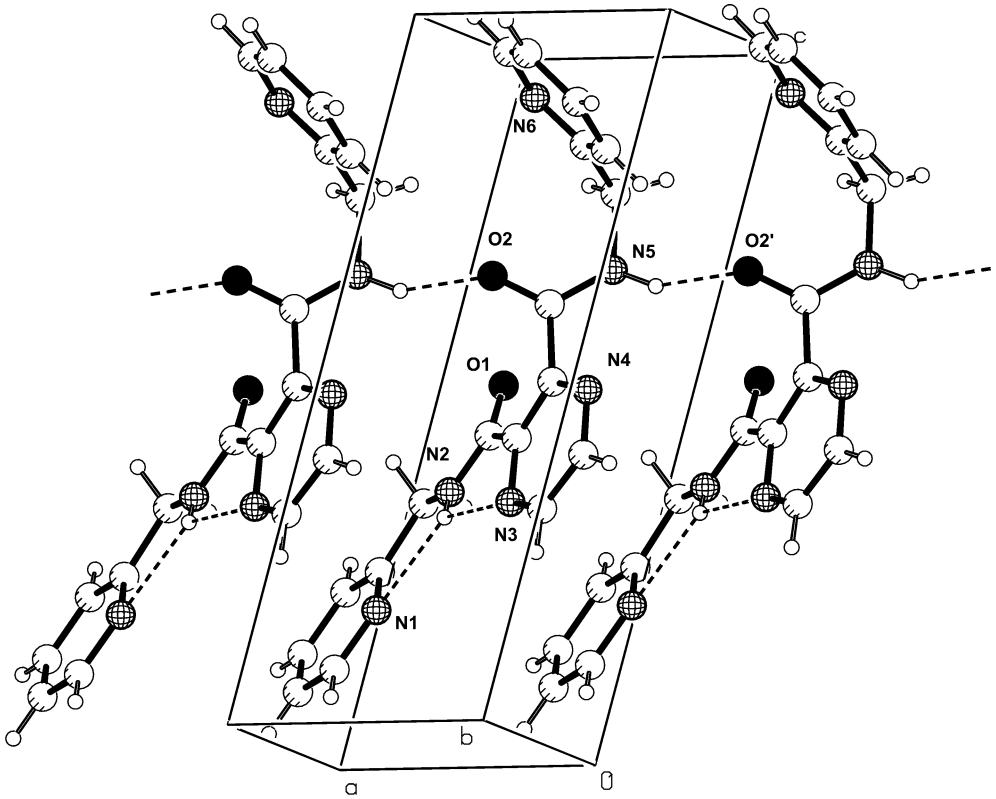

Figure 1. Crystal packing of the ligand H_2L. Dashed lines indicate the intra- and intermolecular hydrogen bonds involving the amide N−H atom, the pyridine N atom, and one of the C═O oxygen atoms (details given in Table 2).

{[Cu$_4$(LH)$_4$](ClO$_4$)$_4$}·5CH$_3$OH·4H$_2$O (2). A solution of H_2L (0.054 g; 0.156 mmol) in 6 mL of CH_2Cl_2 was introduced into a 13 mm diameter glass tube and layered with CH_3OH (2 mL and 3 drops of water), used as a buffer zone. A solution of $Cu(ClO_4)_2$·$6H_2O$ (0.054 g; 0.156 mmol) in CH_3OH (5 mL) was then added gently to avoid possible mixing. The glass tube was sealed with a perforated Parafilm and left at room temperature. The formation of green needlelike crystals was observed after a few days (yield: 56 mg, 77%), which on exposure to air immediately lost solvent. Anal. Calcd for $C_{72}Cu_4H_{60}Cl_4N_{24}O_8$·$4H_2O$: C, 40.92; H, 3.24; N, 15.91. Found: C, 40.84; H, 3.13; N, 15.48.

{[Ni$_4$(LH)$_4$]Cl$_4$}·5CH$_3$CN·13H$_2$O (3). A 0.054 g amount of H_2L (0.156 mmol) and 0.045 g of $NiCl_2$·$6H_2O$ (0.156 mmol) were added to 10 mL of CH_3CN. A 5 mL volume of CH_3CN containing 0.312 mmol of triethylamine was then added followed by 5 mL of methanol. The mixture was refluxed for 5 h and then left to cool and for the solvent to evaporate slowly. After several days brown rodlike crystals appeared (yield: 56 mg, 77%), which on exposure to air immediately lost solvent. Anal. Calcd for $C_{72}H_{60}Cl_4N_{24}Ni_4O_8$·$6H_2O$: C, 46.14; H, 3.87; N, 17.94. Found: C, 46.01; H, 3.97; N, 17.87.

X-ray Crystallography. Intensity data for crystals of ligand H_2L (0.50 × 0.20 × 0.08 mm^3), complex **1** (0.08 × 0.08 × 0.05 mm^3), complex **2** (0.50 × 0.15 × 0.08 mm^3), and complex **3** (0.5 × 0.18 × 0.13 mm^3) were collected at 153 K on a Stoe image plate diffraction system,[8] using Mo Kα graphite monochromated radiation: image plate distance, 70 mm; ϕ oscillation, scans 0−180 or 0−200°; step $\Delta\phi = 1°$; 2θ range 3.27−52.1°; $d_{max}-d_{min} = 12.45-0.81$ Å. The structures were solved by direct methods using the program SHELXS-97.[9] Refinement and all further calculations were carried out using SHELXL-97.[10] For H_2L the H atoms were located from difference maps and refined isotropically. In complexes **1**−**3** the H atoms were either included in calculated positions and treated as riding atoms using SHELXL default parameters or, if they could be located from Fourier difference maps, they were held fixed with U_{iso} values = $1.5U_{eq}$(Ow). For complex **1** only a very small crystal was available and only 1/3 of the reflections can be considered to be observed ($I > 2\sigma(I)$). The amide hydrogen atom H2 could be located in a Fourier difference synthesis as a small positive electron density peak between atoms O1 and O2. However, it was finally included in the calculated position riding on atom O2. The non-H atoms were refined anisotropically, using weighted full-matrix least-squares on F^2. For complex **2** one molecule of methanol and four water molecules per molecule of complex were located from Fourier difference maps. The remaining diffuse electron density was equated to four further molecules of methanol using the SQUEEZE routine in PLATON.[11] For complex **3** 5 molecules of CH_3CN and 13 water molecules could be located per molecule of complex. The molecular structure and crystallographic numbering schemes are illustrated in the PLATON[11] Figures 1−4 and in the Supporting Information (Figures S1−S4). Further crystallographic data are summarized in Table 1. Selected bond lengths and bond angles for ligand H_2L and complexes **1**−**3** are given in Tables 2−5, respectively.

Results and Discussion

Spectral Characterization. The infrared spectra of the ligand and the complexes are given in Table 6. The free ligand, H_2L, shows the characteristic bands (in KBr) for amides groups at 3405 and 3206 cm^{-1}, those for the C═O

(8) *IPDS Software*; Stoe & Cie GmBH: Darmstadt, Germany, 2000.
(9) Sheldrick, G. M. SHELXS-97 Program for Crystal Structure Determination. *Acta Crystallogr.* **1990**, *A46*, 467.
(10) Sheldrick, G. M. *SHELXL-97*; Universität Göttingen: Göttingen, Germany, 1999.
(11) Spek, A. L. PLATON. *Acta Crystallogr*. **1990**, *A46*, C-34.

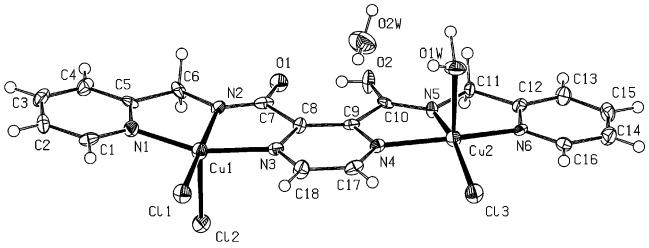

Figure 2. Crystal structure of complex $[Cu_2(LH)(Cl_3)(H_2O)]\cdot H_2O$ (**1**), showing the numbering scheme and the thermal ellipsoids at 50% probability.

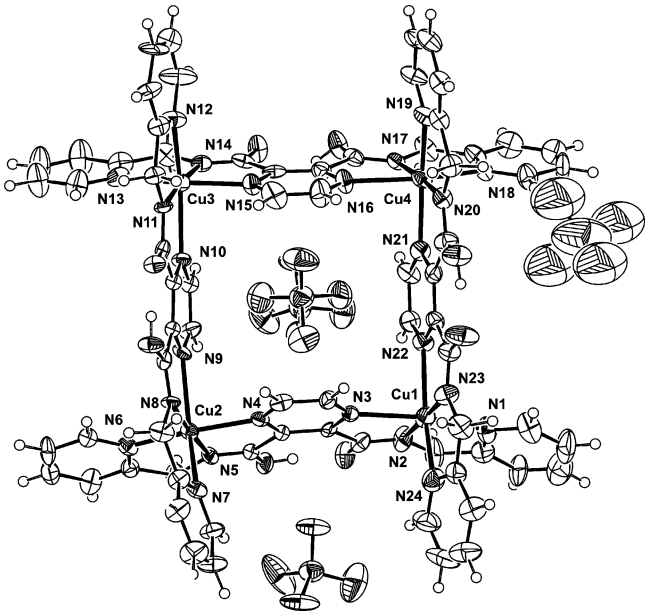

Figure 3. Crystal structure of complex $\{[Cu_4(LH)_4](ClO_4)_4\}\cdot 5CH_3OH\cdot 4H_2O$ (**2**), showing the numbering scheme and the thermal ellipsoids at 50% probability. The solvent and water molecules of crystallization have been omitted for clarity.

stretching vibrations at 1676 and 1665 cm^{-1}, and those for the C−N stretching vibrations at 1534 and 1519 cm^{-1}. In the crystal there are two different types of hydrogen bonds, as shown in Figure 1. There is an intramolecular bifurcated hydrogen bond involving the amide hydrogen atom and pyridine and pyrazine nitrogen atoms and an intermolecular hydrogen bond involving an amide hydrogen atom and a carbonyl O atom of a symmetry-related molecule. The essential difference between these two hydrogen bonds is that the intermolecular hydrogen bond can be broken by dilution with nonpolar solvents. The occurrence and nature of such hydrogen bonding can often be detected by comparing the IR spectra measured in the solid (KBr or Nujol mull) or pure liquid state, with that measured in dilute solution in a nonpolar solvent, such as CH_2Cl_2.[12] The IR spectrum of H_2L was therefore recorded in dichloromethane and indicated that the vibrations associated with the intramolecular hydrogen bond are those appearing at 3405, 1676, and 1519 cm^{-1} (KBr pellet). Hence, the vibrations at 3206, 1665, and 1534 cm^{-1} are due to the intermolecular hydrogen-bonding effect.

(12) Meloan, C. E. *Elementary Infrared Spectroscopy*, 1st ed.; Macmillan Co.: New York, 1963; p 120.

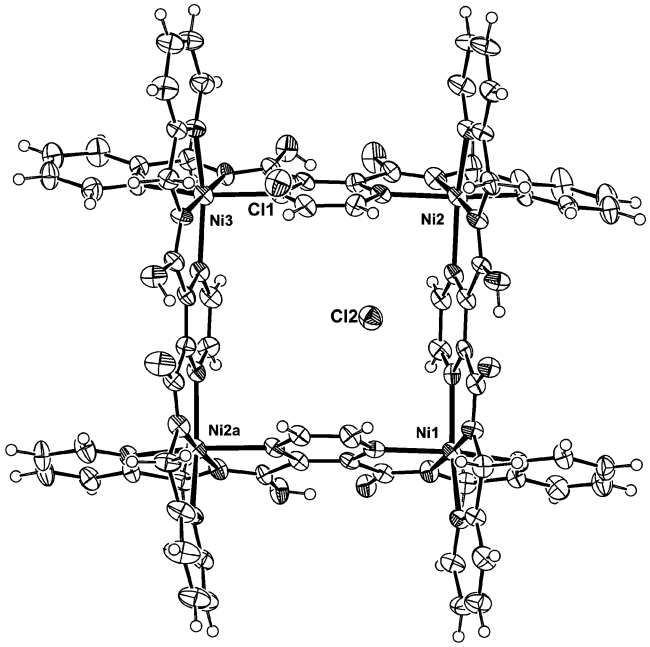

Figure 4. Crystal structure of complex $\{[Ni_4(LH)_4]Cl_4\}\cdot 5CH_3CN\cdot 13H_2O$ (**3**), showing the numbering scheme and the thermal ellipsoids at 50% probability. Symmetry operation a: $1 - x, y, -z + 0.5$. The solvent and water molecules of crystallization, and atoms $Cl1^a$ and $Cl2^a$ have been omitted for clarity.

The IR spectra for the complexes clearly indicate that the ligand is coordinated to the metal with two $\nu_{C=O}$ absorption bands significantly displaced above and below the frequency of 1676 cm^{-1} observed for the free ligand. These two bands appear at 1690 and 1608 cm^{-1} for complex **1**, at 1688 and 1644 cm^{-1} for complex **2**, and at 1697 and 1607 cm^{-1} for complex **3**. On coordination the ligand is negatively charged and contains a deprotonated amide anion, which is stabilized by a hydrogen bond to an adjacent amide group (Scheme 1).

The ESI-MS data for complex **1** in H_2O/CH_3OH indicated the presence of three peaks: *m*/*z* 447.36 corresponds to cation $[(CuHL)Cl]H^+$, *m*/*z* 545.35 corresponds to cation $[(Cu_2HL)Cl_2]^+$, and *m*/*z* 991.71 corresponds to cation $[(Cu_3HL_2)Cl_3]^+$ (a possible oligomer). The ESI-MS data for complex **2** in H_2O/CH_3OH show the presence of the grid complex as well as some other smaller fragments: *m*/*z* 410.90, $[CuHL]^+$; *m*/*z* 759.27, $\{[Cu(HL)_2]^+H^+\}^+$; *m*/*z* 820.80, $\{[(CuL)_2] + H^+\}^+$; *m*/*z* 921.25, $[(CuHL)_4(ClO_4)_2]^{2+}$ (tetranuclear grid).

The ESI-MS data for complex **3** in H_2O/CH_3OH show the presence of the grid complex and fragments of smaller and larger oligomers: *m*/*z* 553.21, $[(NiHL)_4Cl]^{3+}$ (tetranuclear grid); *m*/*z* 669.33, $[(Ni_4HL_5)HCl]^{2+}$ (tetranuclear oligomer); *m*/*z* 754.41, $[(NiHL_2)H^+]^+$ (a monomer complex formed by two ligands with one ion of Ni^{2+}); *m*/*z* 829.31, $[[(NiHL)_4Cl]^{3+} - H^+]^{2+}$ (tetranuclear grid); *m*/*z* 1003.50, $[Ni_4HL_5Cl]^{2+}$ (larger oligomer); *m*/*z* 1206.02, $\{[Ni_5HL_6Cl]^{3+} - H^+\}^{2+}$ (the largest oligomer).

Structural Studies. The ligand H_2L exhibits an L-shaped form in the solid state, Figure 1, with one carboxamide group (C_{pz}, C═O, N, C) almost lying in the plane of the pyrazine ring, while the adjacent carboxamide group is twisted out of the plane of the pyrazine ring. The relevant torsion angles

Table 1. Crystallographic Data for Ligand H_2L and Complexes **1**−**3**

	H_2L	$[Cu_2(LH)(Cl_3)(H_2O)]\cdot H_2O$ (**1**)	$\{[Cu_4(LH)_4](ClO_4)_4\}\cdot 5CH_3OH\cdot 4H_2O$ (**2**)	$\{[Ni_4(LH)_4]Cl_4\}\cdot 5CH_3CN\cdot 13H_2O$ (**3**)
chemical formula	$C_{18}H_{16}N_6O_2$	$C_{18}H_{19}Cl_3Cu_2N_6O_4$	$C_{77}H_{86}Cl_4Cu_4N_{24}O_{33}$	$C_{82}H_{101}Cl_4N_{29}Ni_4O_{21}$
fw	348.37	616.82	2271.66	2205.56
a, Å	4.9882(7)	8.6859(7)	17.1515(14)	16.3388(10)
b, Å	12.079(2)	28.060(2)	17.7507(13)	29.754(2)
c, Å	14.454(2)	9.5334(9)	19.3333(15)	20.8571(12)
α, deg	107.082(18)	90	67.336(8)	90
β, deg	98.610(18)	107.894(10)	69.786(9)	101.848(7)
γ, deg	97.538(18)	90	71.497(9)	90
V, Å^3	808.8(2)	2211.2(3)	4980.3(7)	9923.6(12)
Z	2	4	2	4
space group	$P\bar{1}$ (No. 2)	$P2_1/a$ (No. 14, cell choice 3)	$P\bar{1}$ (No. 2)	*C*2/*c* (No. 15)
T, K	153(2)	153(2)	153(2)	153(2)
D_{calc}, g cm^{-3}	1.430	1.853	1.515	1.476
λ, Å	0.710 73	0.710 73	0.710 73	0.710 73
μ, mm^{-1}	0.099	2.326	1.041	0.937
R1(F_o)[a,b]	0.0747	0.0386	0.0828	0.0500
wR2(F_o^2)[a,c]	0.1829	0.0965	0.2065	0.1009

[a] Observed data $I > 2\sigma(I)$. [b] $R1 = \sum||F_o| - |F_c||/\sum|F_o|$. [c] $wR2 = [\sum w(|F_o^2| - |F_c^2|)^2/\sum wF_o^4]^{1/2}$.

Table 2. Selected Bond Lengths (Å) and Angles (deg), Torsion Angles (deg), and Hydrogen Bonding (Å, deg) for H_2L[a]

C6−N2	1.431(6)	C11−N5	1.462(5)
N2−C7	1.345(6)	N5−C10	1.339(5)
C7−O1	1.227(5)	C10−O2	1.227(5)
C7−C8	1.491(7)	C10−C9	1.515(6)
C8−C9	1.384(6)		

C6−N2−C7	124.1(4)	C11−N5−C10	119.9(4)
N2−C7−C8	114.9(4)	N5−C10−C9	115.2(4)
C7−C8−C9	123.1(4)	C10−C9−C8	124.7(4)
C6−N2−C7−C8	−174.4(4)	C11−N5−C10−C9	−175.2(4)
N2−C7−C8−C9	−173.4(3)	C8−C9−C10−N5	−137.4(4)

D−H···A	D−H	H···A	D···A	D−H···A
N2−H2N···N1	0.74(4)	2.29(5)	2.598(6)	106(4)
N2−H2N···N3	0.74(4)	2.23(5)	2.667(5)	118(4)
N5−H5N···O2^i	1.01(4)	1.86(4)	2.787(5)	151(3)

[a] Symmetry operation i = −1 + *x*, *y*, *z*.

Table 3. Selected Bond Lengths (Å) and Angles (deg) for Complex **1**

Cu1···Cu2	6.848(2)		
Cu1−Cl1	2.232(3)	Cu2−Cl3	2.234(3)
Cu1−Cl2	2.691(3)	Cu2−O(1W)	2.244(8)
Cu1−N1	2.009(9)	Cu2−N6	2.011(9)
Cu1−N2	1.934(9)	Cu2−N5	1.930(9)
Cu1−N3	2.065(9)	Cu2−N4	2.065(9)
O1−C7	1.293(13)	O2−C10	1.280(12)
N2−C7	1.279(15)	N5−C10	1.286(14)

N1−Cu1−Cl1	100.4(3)	N6−Cu2−Cl3	98.8(3)
N1−Cu1−Cl2	92.8(3)	N6−Cu2−O1W	96.7(3)
N2−Cu1−Cl1	171.9(3)	N5−Cu2−Cl3	162.3(3)
N2−Cu1−Cl2	85.3(3)	N5−Cu2−O1W	97.3(3)
N3−Cu1−Cl1	97.8(2)	N4−Cu2−Cl3	97.2(2)
N3−Cu1−Cl2	94.3(2)	N4−Cu2−O1W	93.4(3)
Cl1−Cu1−Cl2	102.3(1)	Cl3−Cu2−O1W	100.2(2)
N1−Cu1−N2	82.0(4)	N6−Cu2−N5	81.8(4)
N1−Cu1−N3	158.6(4)	N6−Cu2−N4	159.3(3)
N2−Cu1−N3	78.4(4)	N5−Cu2−N4	79.0(3)

D−H···A	D−H	H···A	D···A	D−H···A
O2−H2··O1	0.84	1.56	2.40(1)	175

are given in Table 2. In the crystal symmetry-related molecules are linked by an intermolecular hydrogen bond to form a 1D hydrogen bonded polymer; see Figure 1 and Table 2. When the ligand H_2L coordinates to two metals ions, it becomes negatively charged, HL^-, and is stabilized by a hydrogen bond to the adjacent neutral amide tautomer. The idealized situation is shown in Scheme 1i. In the binuclear copper complex **1**, which was formed by the reaction of H_2L with $CuCl_2\cdot 2H_2O$, Figure 2, the bond lengths and angles involving the two amide moieties [average C−O distance 1.29(1) Å, average C−N distance 1.28(1) Å] indicate that the situation in the crystal resembles that in Scheme 1ii. Selected bond distances and angles and details concerning

Table 4. Selected Bond Lengths (Å) and Angles (deg) and Dihedral Angles[a] (deg) for Complex **2**

Cu1···Cu2	7.010(2)	Cu2···Cu3	7.387(2)
Cu1···Cu3	10.065(2)	Cu2···Cu4	10.187(2)
Cu1···Cu4	7.080(2)	Cu3···Cu4	7.169(2)
Cu1−N1	2.145(10)	Cu3−N12	2.225(9)
Cu1−N2	1.940(10)	Cu3−N11	1.974(7)
Cu1−N3	2.233(8)	Cu3−N10	2.309(8)
Cu1−N24	2.181(9)	Cu3−N13	2.079(9)
Cu1−N23	1.950(9)	Cu3−N14	1.940(8)
Cu1−N22	2.241(8)	Cu3−N15	2.144(8)
Cu2−N6	2.039(9)	Cu4−N18	2.229(8)
Cu2−N5	1.935(8)	Cu4−N17	1.985(8)
Cu2−N4	2.129(8)	Cu4−N16	2.314(8)
Cu2−N7	2.293(7)	Cu4−N19	2.105(9)
Cu2−N8	1.993(8)	Cu4−N20	1.955(8)
Cu2−N9	2.387(7)	Cu4−N21	2.156(9)

N1−Cu1−N3	154.5(4)	N12−Cu3−N10	152.6(3)
N24−Cu1−N22	155.0(4)	N13−Cu3−N15	159.7(3)
N2−Cu1−N23	178.9(4)	N11−Cu3−N14	174.1(3)
N2−Cu1−N22	86.4(3)	N10−Cu3−N15	88.3(3)
N6−Cu2−N4	158.8(3)	N18−Cu4−N16	152.2(3)
N7−Cu2−N9	148.9(3)	N19−Cu4−N21	157.3(3)
N5−Cu2−N8	176.0(3)	N17−Cu2−N20	175.3(4)
N4−Cu2−N9	85.8(3)	N16−Cu4−N21	87.4839
py1∧py2	82.2(5)	py2∧py3	87.8(6)
py1∧py3	39.8(6)	py2∧py4	31.2(5)
py1∧py4	84.6(6)	py3∧py4	84.5(6)

[a] py1 pyrazine ring involving atoms N3, N4; py2 pyrazine ring involving atoms N9, N10; py3 pyrazine ring involving atoms N15, N16; py4 pyrazine ring involving atoms N21, N22.

Table 5. Selected Bond Lengths (Å) and Angles (deg) and Dihedral Angles[a] (deg) for Complex **3**

Ni1···Ni2	6.988(1)	Ni2···Ni3	6.948(1)
Ni1···Ni3	9.786(2)	Ni2···Ni2i	9.921(2)
Ni1−N1	2.088(5)	Ni2−N12	2.078(5)
Ni1−N2	1.979(4)	Ni2−N11	1.983(4)
Ni1−N3	2.128(5)	Ni2−N10	2.107(5)
Ni2−N6	2.094(4)	Ni3−N7	2.065(4)
Ni2−N5	1.986(4)	Ni3−N8	2.000(4)
Ni2−N4	2.131(5)	Ni3−N9	2.114(5)

N1−Ni1−N3	156.9(2)	N7−Ni3−N9	155.8(2)
N2−Ni1−N2i	177.8(3)	N8−Ni3−N8i	179.3(3)
N3−Ni1−N3i	88.8(2)	N9−Ni3−N9i	94.1(2)
N6−Ni2−N4	156.2(2)	N5−Ni2−N11	176.4(2)
N12−Ni2−N10	156.6(2)	N4−Ni2−N10	90.1(2)
py1∧py2	84.5(3)	py1∧py1^i	85.5(3)
py1∧py2^i	33.1(3)	py2∧py2^i	86.9(39

[a] py1 parazine ring involving atoms N3, N4; py2 pyrazine ring involving atoms N9, N10. Symmetry operation i = 1 − *x*, *y*, 0.5 − *z*.

Table 6. Infrared Spectra (cm^{-1}) of H_2L and Complexes **1**−**3**

compd	ν_{N-H}	$\nu_{C=O}$	ν_{C-N}	other bands
H_2L (KBr disk)	3405 (s), 3206 (s)	1676 (vs), 1665 (vs)	1534 (vs), 1519 (vs)	3050 (m), 1592 (s), 1570 (vs), 1474 (s), 1438 (s), 996 (s), 773 (s), 617 (m)
H_2L (in CH_2Cl_2)	3397 (w)	1681 (vs)	1515 (vs)	3052 (vs), 1594 (s), 1572 (m), 1438 (m), 999 (w), 752 (s)
$[Cu_2(LH)(Cl_3)H_2O]\cdot H_2O$ (**1**)		1690 (w),1608 (vs)		3445 (b, s), 1565 (vs), 1463 (vs), 1383 (vs), 1156 (vs), 1053 (vs), 1026 (vs), 873 (b, vs), 706 (s)
$\{[Cu_4(LH)_4](ClO_4)_4\}\cdot 5CH_3OH\cdot 4H_2O$ (**2**)		1688 (s), 1644 (vs)		3429 (b, s), 1615 (vs), 1579 (s), 1470 (s), 1389 (s), 1088 (vs), 928 (m), 859 (w), 765 (m), 718 (m), 625 (s)
$\{[Ni_4(LH)_4]Cl_4\}\cdot 5CH_3CN\cdot 13H_2O$ (**3**)		1696 (s), 1607 (vs)		3400 (b, s), 1564 (vs), 1482 (vs), 1409 (vs), 1374 (vs), 1286 (s), 1241 (s), 1151 (vs), 1050 (vs), 1021 (vs), 884 (s), 763 (s), 704 (s)

the intramolecular hydrogen bond are given in Table 3. The same situation is observed in complexes **2** and **3** and in the binuclear copper complex formed using a similar ligand, (*N*,*N*′-bis(2-pyridyl)ethyl)-2,3-pyrazinecarboxamide.[13] The latter possesses one more carbon atom in each of the side chains, compared to H_2L. In **1** atom Cu1 has a distorted square pyramidal (SP) geometry (Addison parameter,[14] $\tau = 0.22$), while atom Cu2 has perfect SP geometry ($\tau = 0.05$). The copper atoms are separated by 6.848(2) Å and are coordinated to one pyridine, one amide, and one pyrazine N atom. The coordination sphere of Cu1 is completed by two Cl atoms, while that of Cu2 is completed by one Cl atom and a water molecule. On coordination the entire ligand is now planar to within 0.04 Å. The average $Cu-N_{am}$ (am = amide) bond distance is 1.932(5) Å, which is shorter than the average $Cu-N_{py}$ (py = pyridine) distance of 2.010(5) Å, which in turn is shorter than the average $Cu-N_{pz}$ (pz = pyrazine) distance 2.065(5) Å. A similar trend was found for the Cu−N bond distances in the above-mentioned complex studied by Fleischer et al.,[13] however, with some differences in the absolute values of the $Cu-N_{am}$ and $Cu-N_{pz}$ bond lengths of 1.956 Å (longer than in **1**) and 2.022 Å (shorter than in **1**), respectively.

In the crystal symmetry-related molecules are linked by hydrogen bonds involving the coordinated water molecule, the coordinated chlorine atoms, and the water molecule of crystallization. A 2D hydrogen-bonded double-layer-like arrangement is formed extending in the ac plane.

The reaction of H_2L with $Cu(ClO_4)_2\cdot 6H_2O$ and $NiCl_2\cdot 6H_2O$ led to the formation of a Cu^{II} cationic [2 × 2] grid (**2**) and a Ni^{II} cationic [2 × 2] grid (**3**), respectively**.** The X-ray crystal structure analyses of **2** and **3** (Figures 3 and 4) reveal that in both cases the ligands are divided into pairs, one of which lies above and the other below the mean plane through the four metal ions, giving two novel [2 × 2]G grids. Interestingly the Ni^{II} [2 × 2]G grid possesses C_2 symmetry. All four Cu^{II} or Ni^{II} atoms are octahedrally coordinated by two pyridine, two amide, and two pyrazine N atoms and so occupy the corners of a [2 × 2] grid with average edge lengths Cu···Cu 7.162(1) Å and Ni···Ni 6.968(1) Å. The former distance is significantly longer than the Cu···Cu distance in **1**, 6.878(2) Å. The average metal−metal diagonal distances are 10.126(1) Å for **2** and 9.854(1) Å for **3**. The grids are not perfectly square as can be seen by the dihedral angles involving the adjacent pyrazine rings, 82.2(5)−87.8(6)° for **2** and 84.5(3)−86.9(3)° for **3**. The ligand molecules on opposite sides of the grids are also inclined to one another. This is shown by the dihedral angles involving the opposing pyrazine rings, 39.8(6) and 31.2(5)° for **2** and 33.1(3)° for **3**. This arrangement is clearly seen in Figures 3 and 4, and details are given in Tables 4 and 5. The strain in the molecule is also indicated by the metal to nitrogen bond distances in **2**, which are significantly longer than those observed for the binuclear complex **1**. The $Cu-N_{am}$ distances vary from 1.935 to 1.993 Å, the $Cu-N_{py}$ distances from 2.039 to 2.181 Å, and the $Cu-N_{pz}$ distances from 2.225 to 2.389 Å. In **3** the average nickel−nitrogen bond distances, $Ni-N_{am} = 1.981(3)$ Å, $Ni-N_{py} = 2.083(4)$ Å, and $Ni-N_{pz} = 2.118(4)$ Å, are also longer than values observed in similar complexes. For example, the nickel complex formed with the ligand *N*,*N*′-bis(2-pyridylmethyl)malonic diamide,[15] where the average $Ni-N_{am}$ distance is 1.854 Å and the average $Ni-N_{py}$ distance is 1.914 Å. The $Ni-N_{pz}$ distance is significantly longer than normally observed; for example, an average distance of 2.013 Å was observed in two nickel complexes with the ligand tetrakis(2-pyridyl)pyrazine.[16]

Four ClO_4^- and four Cl^- ions are present to equilibrate the charges in **2** and **3**, respectively. In **2** the faces of the grid are protected by two encapsulated perchlorate anions, one on either side, as seen in Figure 3. The other two ClO_4^- anions are located in the spaces between the "wings", that is, the outer pyridine rings of the ligands. In the case of the nickel complex **3** it can be seen that two Cl^- ions are encapsulated, one on either side of the grid, and that the remaining two sit rather asymmetrically, on either side of the grid entrances, Figure 4. In both complexes the anions appear to be held in place by a certain number of weak C−H···O(perchlorate) interactions in **2** and C−H···Cl^- and O−H(solvent water)···Cl^- interactions in **3**. Encapsulation of a single anion by molecular squares,[17] or triangles,[18] gridlike complexes,[19,20] a molecular pentagon,[21] and funnel-

(13) (a) Fleischer, E. B.; Lawson, M. B. *Inorg. Chem.* **1972**, *11*, 2772. (b) Fleischer, E. B.; Jeter, D.; Florian, R. *Inorg. Chem.* **1974**, *13*, 1042.
(14) Addison, A. W.; Rao, T. N.; Reedjik, J.; van Rijn, J.; Verschoor, C. G. *J. Chem. Soc., Dalton Trans.* **1984**, 1349.
(15) Comba, P.; Goll, W.; Nuber, B.; Vamagy, K. *Eur. J. Inorg. Chem.* **1998**, 2041.
(16) Graf, M.; Stoeckli-Evans, H.; Escuer, A.; Vicente. R. *Inorg. Chim. Acta* **1997**, *257*, 89.
(17) (a) Campos-Fernández, C. S.; Clérac, R.; Dunbar, K. R. *Angew. Chem., Int. Ed.* **1999**, *38*, 3477. (b) Bu, X.-H.; Morishita, H.; Tanaka, K.; Biradha, K.; Furusho, S.; Shionoya, M. *Chem. Commun.* **2000**, 971. (c) Schweiger, W.; Seidel, S. R.; Arif, A. M.; Stang, P. J. *Inorg. Chem.* **2002**, *41*, 2556. (d) Whiteford, J. A.; Lu, C. V.; Stang, P. J. *J. Am. Chem. Soc.* **1997**, *119*, 2524.
(18) (a) Schnebeck, R.-D.; Freisinger, E.; Lippert, B. *Chem. Commun.* **1999**, 675. (b) Schnebeck, R.-D.; Freisinger E.; Glahé, F.; Lippert, B. *J. Am. Chem. Soc.* **2000**, *122*, 1381. (c) Schweiger, W.; Seidel, S. R.; Arif, A. M.; Stang, P. J. *Angew. Chem., Int. Ed.* **2001**, *40*, 3467.
(19) Krämer, R.; Kovbasyuk, L.; Pritzkow, H. *New. J. Chem.* **2002**, *26*, 516.

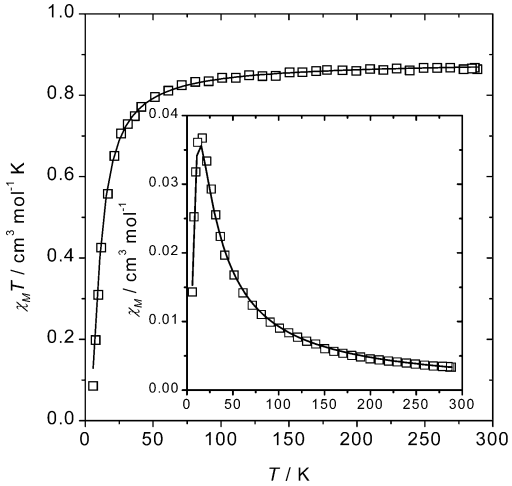

Figure 5. Temperature dependence of $\chi_M T$ and χ_M (insert), for complex **1**. The solid curves (—) represent the best fits, as discussed in the text.

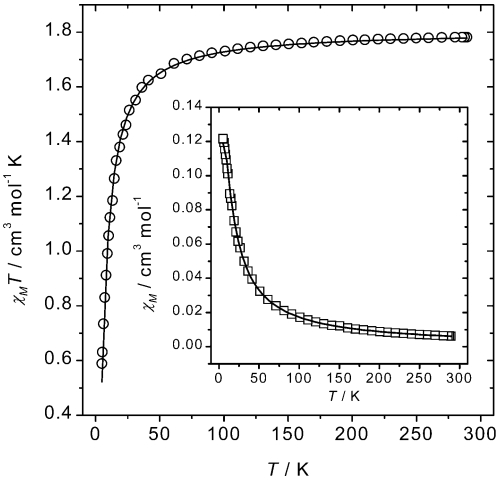

Figure 6. Temperature dependence of $\chi_M T$ and χ_M (insert), for complex **2**. The solid curves (—) represents the best fits, as discussed in the text.

shaped tri- and hexanuclear complexes,[22] has been observed previously. The encapsulation of two or more anions is rarer.[17d,18b,22,23] Two examples that also involve pyrazine derivatives are zinc(II) molecular squares. One was prepared with the ligand 2,5-bis(2,2′-bipyridin-6-yl)pyrazine, and the other with the chiral ligand 2,5-bis((*R*,*R*)-[4′,5′]pineno-2,2′-bipyridin-6-yl)pyrazine.[23] In each case eight PF_6^- anions are required to neutralize the charges, and as in complexes **2** and **3**, one is located above the square and a second below.

Magnetic Properties. Variable-temperature magnetic data were obtained for **1**−**3** using a 0.1 T field in the temperature range 4−300 K. The variation of χ_M (insert) and $\chi_M T$ vs T for the binuclear complex **1** is shown in Figure 5. χ_M increases from 0.0030 cm^3 mol^{-1} at 288.67 K to a maximum of 0.0367 cm^3 mol^{-1} at 16.67 K and then decreases to 0.0143 cm^3 mol^{-1} at 5.95 K. $\chi_M T$ varies from 0.8647 cm^3 mol^{-1} K at 288.67 K to 0.0612 cm^3 mol^{-1} K at 16.67 K and then falls to 0.085 cm^3 mol^{-1} K at 5.95 K. The susceptibility data were fitted to a Bleaney−Bowers expression[24] for a binuclear Cu_2 entity, derived from the Hamiltonian

$$H = -J(S_1S_2) \qquad (1)$$

The best least-squares fit gave parameters $J = -15.07$ cm^{-1} and $g = 2.17$. TIP was assumed as 100×10^{-6} cm^3 mol^{-1}. The agreement factor $R = \sum[\chi_M^{exp} - \chi_M^{calc}]^2/\sum[\chi_M^{exptl}]^2$ was 5.15×10^{-6}. The J value obtained corresponds to a weak antiferromagnetic coupling between the adjacent copper(II) ions.

The magnetic behavior of the Cu^{II} complex **2** is shown in Figure 6 as the variation of χ_M (insert) and $\chi_M T$ vs T. χ_M increases from 0.00616 cm^3 mol^{-1} at 289.31 K to a maximum of 0.1222 cm^3 mol^{-1} at 4.84 K. $\chi_M T$ varies from 1.78 cm^3 mol^{-1} K at 289.31 K to 0.59 cm^3 mol^{-1} K at 4.84 K. The susceptibility data were fitted to a theoretical expression[25] for a square Cu_4 entity, derived from the Hamiltonian

$$H = -J(S_1S_2 + S_1S_4 + S_2S_3 + S_3S_4) \qquad (2)$$

where $J = J_{12} = J_{14} = J_{23} = J_{34}$.

Least-squares fitting of the data gave $J = -5.87$ cm^{-1} and $g = 2.19$. TIP was assumed as 200×10^{-6} cm^3 mol^{-1}. The agreement factor $R = \sum[\chi_M^{expt} - \chi_M^{calc}]^2/\sum[\chi_M^{expt}]^2$ was 2.1×10^{-4}. The J value obtained corresponds to a weak antiferromagnetic coupling between adjacent copper(II) ions.

For complex **3** (Figure S5) χ_M increases from 0.0157 cm^3 mol^{-1} at 290.6 K to a value of 0.315 cm^3 mol^{-1} at 4.62 K. χ_MT varies from 4.57 cm^3 mol^{-1}K at 290.6 K to 1.45 cm^3 mol^{-1}K at 4.62 K. Using the same Hamiltonian as above, eq 2, and the expression for the molar susceptibility as reported by Ribas et al.,[26] the best fit parameters are $J = -2.64$ cm^{-1} and $g = 2.17$. TIP was assumed as 400×10^{-6} cm^3 mol^{-1}. The agreement factor $R = \sum[\chi_M^{exp} - \chi_M^{calc}]^2/\sum[\chi_M^{exptl}]^2$ was 2.7×10^{-4}. The J value obtained again corresponds to a weak antiferromagnetic coupling between the adjacent nickel(II) ions.

Magneto−Structural Correlations: DFT Calculations. For complexes **1**−**3** there are theoretically two possible magnetic pathways between the two metal ions (Cu^{II} or Ni^{II}): either via the amide-to-amide hydrogen-bond or via the pyrazine moiety of the bridging ligand. The former has been shown to be very inefficient;[27] for the later, previous work has established that pyrazine, and pyrazine derivatives in general, are also relatively inefficient exchange bridging ligands. They exhibiting low exchange J values of between 0 and −15 cm^{-1}.[16,28] However, a J value as large as −30.5 cm^{-1} was found for a binuclear Cu^{II} complex with the ligand tetrakis(2-pyridyl)pyrazine.[16] An interesting problem when comparing the binuclear complex **1** and the tetranuclear-grid

(20) Bassani, D. M.; Lehn, J.-M.; Fromm, K.; Fenske, D. *Angew. Chem., Int. Ed.* **1998**, *37*, 2364.
(21) Campos-Fernández, C. S.; Clérac, R.; Koomen, J. M.; Russell, D. H.; R.; Dunbar, K. R. *J. Am. Chem. Soc.* **2001**, *123*, 773.
(22) Schnebeck, R.-D.; Freisinger, E.; Lippert, B. *Angew. Chem., Int. Ed.* **1999**, *38*, 168.
(23) Bark, T.; Düggeli, M.; Stoeckli-Evans, H.; von Zelewsky, A. *Angew. Chem., Int. Ed.* **2001**, *40*, 2848.
(24) Bleaney, B.; Bowers, K. D. *Proc. R. Soc. London, Ser. A* **1952**, *214*, 451.
(25) Castro, I.; Sletten, J.; Calatayud, M. L.; Julve, M.; Cano, J.; Lloret, F.; Caneschi, A. *Inorg. Chem.* **1995**, *34*, 4903.
(26) Ribas, J.; Monfort, M.; Costa, R.; Solans, X. *Inorg. Chem.* **1993**, *32*, 695.

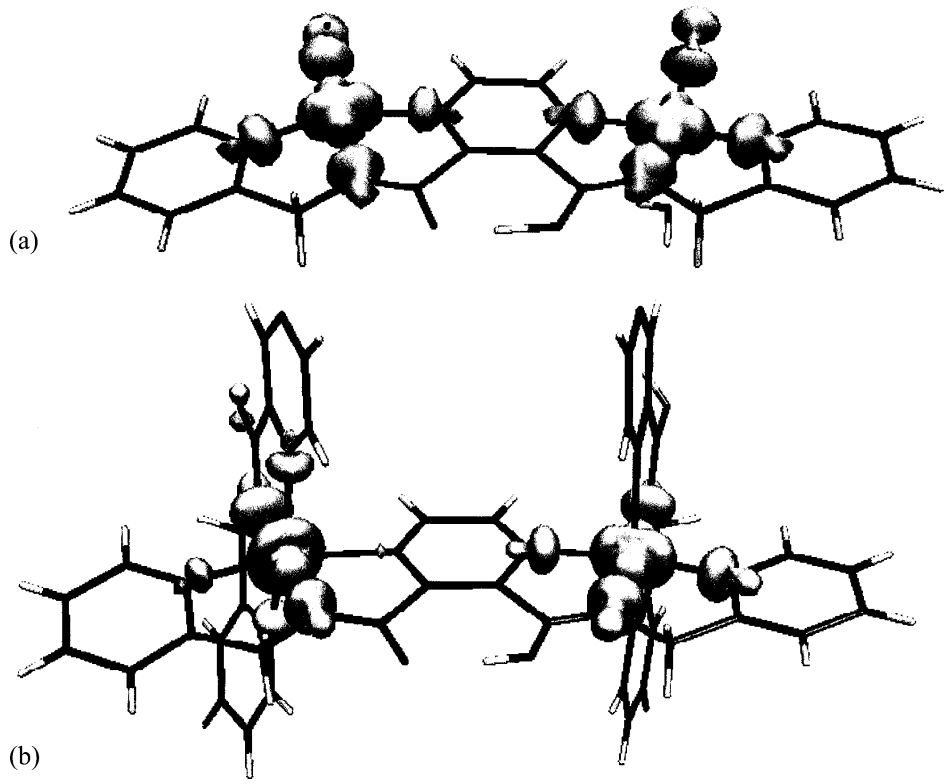

Figure 7. Spin densities for (a) the binuclear complex **1** and (b) the [Cu(1)···Cu(4)] binuclear moiety of the tetranuclear complex **2**.

copper(II) complex **2** is the large difference between the corresponding *J* values as the bridging ligand is the same (-15.07 and -5.87 cm^{-1}, respectively). There are qualitative and quantitative explanations for this phenomenon. From a qualitative point of view, in the binuclear complex **1** the geometry of each copper(II) atom is close to square pyramidal. The Addison parameter, τ,[14] is 0.22 for Cu1 and 0.05 for Cu2. This is in contrast to the tetranuclear complex **2**, which consists of four copper atoms with different and rather distorted octahedra, as can be seen from the Cu−N distances in Table 4. Obviously, from a theoretical point of view, the four *J* coupling constants will be different on each side of the square-grid. However, taking into account the low experimental *J* value, any attempt to find each individual *J* value would be unrealistic. Consequently, one can only compare the average *J* value for **2** to the *J* value for the binuclear complex **1**. Thus, as a qualitative and pictorial explanation, in the binuclear complex **1** the magnetic orbitals of the Cu^{II} atoms are well directed toward the pyrazine moiety, but this is not the case for the grid complex, **2**.

From a quantitative point of view, ab initio calculations have been performed using the B3LYP[29] method as implemented in the GAUSSIAN98 package[30] with the Ahlrichs pVDZ basis set. The binuclear complex **1** was studied using its crystallographic structure. For the tetranuclear Cu^{II} complex **2** the crystallographic structure of one of the Cu−pyrazine−Cu moieties [Cu(1)···Cu(4)] was used as representative of the four copper atoms, owing to their similar but not quite identical structure. The shape of the SOMO orbitals (natural orbital representation) and the associated spin density at various cutoffs were computed. The SOMO's show (Supporting Information, Figures S6 and S7) the presence of ligand components, which is also reflected in the spin density distribution. This indicates that the mechanism of the magnetic interaction between the Cu atoms is of the superexchange type. Plots of the spin density at 0.01 cutoff are shown in Figure 7. These plots and the analysis of the Mulliken spin population of the two systems indicate that the area of high spin density is located on the two Cu atoms, the next area in importance being the atoms directly attached to the Cu atoms (Table 7). The amount of density on the atoms of the O−H···O hydrogen bond and on the C atoms is negligible (1 order of magnitude lower than the smallest

(27) (a) Xie, Y.; Liu, Q.; Jiang, H.; Du, C.; Xu, X.; Yu, M.; Zhu, Y. *New J. Chem.* **2002**, *26*, 176 and references therein. (b) Paine, T. K.; Weyhermuller, T.; Wieghardt, K.; Chaudhuri, P. *Inorg. Chem*. **2002**, *41*, 6538 and references therein. (c) Desplanches, C.; Ruiz, E.; Rodriguez-Fortea, A.; Alvarez, S. *J. Am. Chem. Soc*. **2002**, *124*, 5197. (d) Tercero, J.; Diaz, C.; Ribas, J.; Mahía, J.; Maestro, M. A. *Inorg. Chem*. **2002**, *41*, 5373 and references therein.

(28) Oshio, H.; Nagashima, U., *Inorg. Chem*. **1990**, *29*, 3321 and references therein.

(29) Parr, R. G.; Yang, W. *Density-Functional Theory of atoms and Molecules*; Oxford University Press: New York, 1989.

(30) Frisch, M. J.; Trucks, G. W.; Schlegel, H. B.; Scuseria, G. E.; Robb, M. A.; Cheeseman, J. R.; Zakrzewski, V. G.; Montgomery, J. A., Jr.; Stratmann, R. E.; Burant, J. C.; Dapprich, S.; Millam, J. M.; Daniels, A. D.; Kudin, K. N.; Strain, M. C.; Farkas, O.; Tomasi, J.; Barone, V.; Cossi, M.; Cammi, R.; Mennucci, B.; Pomelli, C.; Adamo, Clifford, C. S.; Ochterski, J.; Petersson, G. A.; Ayala, P. Y.; Cui, Q.; Morokuma, K.; Malick, D. K.; Rabuck, A. D.; Raghavachari, K.; Foresman, J. B.; Cioslowski, J.; Ortiz, J. V.; Baboul, A. G.; Stefanov, B. B.; Liu, G.; Liashenko, A.; Piskorz, P.; Komaromi, I.; Gomperts, R.; Martin, R. L.; Fox, D. J.; Keith, T.; Al-Laham, M. A.; Peng, C. Y.; Nanayakkara, A.; Gonzalez, C.; Challacombe, M.; Gill, P. M. W.; Johnson, B.; Chen, W.; Wong, M. W.; Andres, J. L.; Head-Gordon, M.; Replogle, E. S.; Pople, J. A. *Gaussian 98*, revision A.7; Gaussian, Inc.: Pittsburgh, PA, 1998.

Table 7. Calculated Atom Spin Population for the Binuclear Complex, **1**, and for the [Cu(1)··Cu(4)] Binuclear Moiety of the Tetranuclear Complex, **2**[a]

atom	binuclear **1**	atom	tetranuclear **2**
N1	0.090	N18	0.010
N2	0.108	N19	0.080
Cl(Cl1)	0.137	N17	0.079
N3 (pyrazine)	0.050	N16	0.004
Cu1	0.589	N20	0.125
Cu2	0.582	N21 (pyrazine)	0.051
N4 (pyrazine)	0.071	Cu4	0.657
N6	0.096	Cu1	0.629
N5	0.104	N22 (pyrazine)	0.009
Cl3	0.137	N24	0.029
O1w	0.000	N2	0.139
		N3	0.042
		N23	0.088
		N1	0.048

[a] Values are given for the copper(II) and terminal ligand atoms; for the other atoms the spin density is close to zero. The crystallographic labels of the atoms are given.

spin density of the coordinated atoms). Another interesting consequence of the spin distribution is the presence of nodes in the spin distribution of the atoms of the ligand and the fact that the atoms of the O−H···O hydrogen bond form an isolated island in this spin density map. This suggests that no spin propagation, of the type suggested by Ovchinikov,[31] is possible along the hydrogen bond.

To further evaluate the possibility of propagation of spin along the intramolecular O−H···O hydrogen bond, the SOMO, the spin density map, and the atomic spin distribution were computed using the Mulliken scheme for the experimental model system and the same molecule when the hydrogen of the O−H···O moiety was forced to be perpendicular to the plane of the molecule. The results show that the SOMO, the spin density map, and the spin populations are very much the same for the two molecules, thus also suggesting the absence of magnetic interaction along the O−H···O bond.

The amount of spin delocalization toward the pyrazine nitrogens is nicely correlated in complexes **1** (binuclear) and **2** (tetranuclear) with the respective J values (-15.07 cm^{-1} compared to -5.87 cm^{-1}). In the binuclear complex, **1**, these coefficients are 0.07 and 0.05 whereas in the tetranuclear complex, **2**, they are 0.05 and 0.009 (Table 7). In **1** the difference in magnitude can be correlated to the τ parameters, which are 0.22 and 0.05, respectively. As the distortion in the copper(II) atoms in the tetranuclear complex **2** is greater, this creates a significant asymmetry in the spin density coefficients. It can also be seen that there is a correlation between these spin-density coefficients and the Cu−N_{pz} bond distances. In complex **1** these distances are both 2.065(9) Å, whereas in complex **2** these distances are longer, 2.129(8) and 2.233(8) Å in the moiety studied (representative of all of the Cu−N_{pz} distances which vary from 2.129(8) to 2.387(7) Å).

In conclusion, the spin density (Figure 7 and Table 7) shows that, for the binuclear complex, the global spin electron density is almost entirely centered on the $d_{x^2-y^2}$ orbital for each Cu^{II} ion. The magnetic pathway is thus governed by the $d_{x^2-y^2}$ orbital and the N atoms of the pyrazine bridging ligand. The electron density indicates a relatively good overlap through the corresponding orbital of the pyrazine bridging ligand, giving an appreciable antiferromagnetic coupling, despite the fact that this ligand normally gives a poor superexchange pathway. For the tetranuclear complex, where the bond distances and angles indicate a distorted octahedral geometry (see Table 4), the spin-density distribution is mainly located on one or more d orbital and less efficiently on the N_{pz} atoms of the bridging ligand. This feature strongly reduces the overlap with the orbitals of the pyrazine and diminishes the antiferromagnetic pathway.

For the nickel complex **3** the problem is less complicated as the geometry of all four nickel atoms is the same (Table 5). The free electrons are in the magnetic orbitals d_{z^2} and $d_{x^2-y^2}$; hence, both pathways are involved even if the magnetic superexchange is weak. In this case, for a Ni^{II} ion, the J coupling constant is approximately $1/n{\cdot}n = 1/4$ of the value for the analogous Cu^{II} complex.[32]

Conclusions

The new semiflexible substituted pyrazine ligand H_2L, with two adjacent amide bonds, has been shown to be extremely stable to complexation with copper and nickel ions, as shown by the formation of complexes **1**−**3**. The stability of the amide bond toward metal-catalyzed hydrolysis is thought to be due to the formation of a negatively charged ligand containing a deprotonated amide anion, which is stabilized by a hydrogen bond to the adjacent amide group (Scheme 1). The [2 × 2]G complexes, **2** and **3**, form spontaneously by the self-assembly of eight units: four ligands and four metal ions. The self-assembly of the [2 × 2]G grids complies with the principle of "maximum coordination site occupation".[1] It can also be rationalized in terms of the appropriate design of the ligand and choice of its dimensionality properties, which exclusively leads to the generation of the closed grid structure instead of a coordination polymer. The generation of predetermined gridlike architectures by self-assembly processes, using preprogrammed ligands, provides a unique opportunity to produce complex nanostructures. Another interesting feature of these two complexes is that both are methanol- and water-soluble. With the more flexible ligand of Fleischer et al.,[13] only a Cu^{II} binuclear complex and mononuclear Co^{II} and Ni^{II} complexes were reported.[13] In light of these results, it seems clear that the rigidity of ligand H_2L and the intramolecular hydrogen bond formed with the migrated N−H hydrogen atom play an important role in the formation of the [2 × 2]G grid complexes and that the inclination of the opposing ligands is essential for anion encapsulation. However, the question remains whether the presence of the anions is essential for the formation of the grid complexes as proposed previously.[17a] The grid complexes are water- and methanol-soluble, and the intact tetranuclear complexes could be detected by electrospay mass spectrometry {m/z 921.25, $[(CuHL)_4(ClO_4)_2]^{2+}$ (tetranuclear

(31) Ovchinikov, A. A. *Theor. Chim. Acta* **1978**, *47*, 297.

(32) Kahn, O. *Molecular Magnetism*; VCH Publishers: New York, 1993.

grid); *m*/*z* 553.21, $[(NiHL)_4Cl]^{3+}$ (tetranuclear grid)}. However, in view of the fact that the grid complexes could be formed using two different metals with two very different anions suggests that the formation of the grids is governed primarily by the coordination properties, that is the design, of the ligand. Further studies are underway to explore if larger metallocyclophanes can be constructed by tuning the counterion size and shape.

Acknowledgment. We gratefully acknowledge the financial support of the Swiss National Science Foundation (Grant FN 20-58995.99 to H.S.-E.) and the Spanish Government (Grant BQU2000/0791 to J.R.). We also wish to thank Prof. Joan Novoa (Department de Química Física, Universitat de Barcelona) for helpful discussions.

Note Added in Proof: Hausmann et al.[33] have recently reported the structures of some $Cu(BF_4)_2$ complexes of the same ligand including a [2 × 2] grid; however, no anion encapsulation was observed.

Supporting Information Available: Figures of the structure of the ligand H_2L, the crystal packing in complex **1**, side views of complexes **2** and **3**, magnetic susceptibility data for complex **3**, and the SOMO's molecular orbitals for complexes **1** and **2** and crystallographic data for compounds H_2L and **1**−**3** in CIF format. This material is available free of charge via the Internet at http://pubs.acs.org.

IC030174S

(33) Hausmann, J.; Jameson, G. B.; Brooker, S. *Chem. Commun.* **2003**, 2992.